comparison with $I(s)$ it may be set equal to $\phi(0)$ in the integration, so that, since $\int I(s)\,ds = V_0/U \equiv I$,

$$\epsilon = \lambda\phi(0)/2\sin\theta. \tag{17}$$

On the other hand, if $I(s)$ is the wide curve it may be set equal to $I(0)$ for the integration over $\phi(e)$, so that

$$\epsilon = (U/V_0)\,I(0) = I(0)/I. \tag{18}$$

Equations (17) and (18) express distortion and small-particle broadening respectively. The functional form of the transitions from one to the other depends on the exact shape of $\phi(e)$ and $I(s)$. With the common, but unreliable, Gaussian approximations

$$\phi(e) \doteqdot (2\pi\eta^2)^{-\frac{1}{2}} \exp\{-e^2/2\eta^2\}, \tag{19}$$

and

$$I(s) \doteqdot IE \exp\{-\pi E^2 s^2\}, \tag{20}$$

where η is the root-mean-square stress and E is an order-of-magnitude particle size, equation (15) gives

$$\epsilon \doteqdot E(2\pi\eta^2)^{-\frac{1}{2}} \int_{-\infty}^{\infty} \exp\left\{-e^2\left[\frac{1}{2\eta^2} + \frac{4\pi E^2 \sin^2\theta}{\lambda^2}\right]\right\} de$$
$$= 2E\{4 + 16A_1^2\}^{-\frac{1}{2}}, \tag{21}$$

where

$$A_1 = \sqrt{(2\pi)}\,E\eta\sin\theta/\lambda. \tag{22}$$

Equation (22) is quite analogous to (5), in which $T/p \sim E$, $A \sim A_1$, and the integral has the same limiting values as $\{4 + 16A_1^2\}^{-\frac{1}{2}}$. The decrease of ϵ with increase in A is, however, much more rapid for (21). Other approximations to $\phi(e)$ and $I(s)$ lead to the same general behaviour, but different functional dependence on A. Thus, for sufficiently small values of $\sin\theta/\lambda$, particle-size broadening will always mask distortion broadening; and for sufficiently large values distortion broadening will be predominant. The manner in which the transition takes place will depend on the nature of the distortion and the shape of the crystallites.

References

Lipson, H. & Stokes, A. R. (1943). *Nature, Lond.*, **152**, 20.

Orowan, E. (1942). *Nature, Lond.*, **149**, 643.

Stokes, A. R. & Wilson, A. J. C. (1944*a*). *Proc. Phys. Soc. Lond.* **56**, 174.

Stokes, A. R. & Wilson, A. J. C. (1944*b*). *Proc. Camb. Phil. Soc.* **40**, 197.

Wilson, A. J. C. (1943). *Proc. Roy. Soc.* A, **181**, 360.

Wood, W. A. (1943). *Nature, Lond.*, **151**, 585.

Wood, W. A. & Rachinger, W. A. (1948). *Nature, Lond.*, **162**, 891.

Acta Cryst. (1949). **2**, 222

Diffuse Scattering of X-rays by Ice

By P. G. Owston

*University College, London W.C.*1, *England*

(*Received* 17 *February* 1949)

The diffuse scattering of X-rays by single crystals of ice has been found to be of thermal origin. The existing theory is inadequate to explain the observations, and needs extending to include the effects of vibrations of shorter wave-lengths. The main features of the representation in reciprocal space of the diffuse scattering are as follows:

(1) There is a strong concentration of scattering power immediately round the reciprocal-lattice points, corresponding to rounded isodiffusion contours.

(2) Beyond these regions are weaker bridges, which connect reciprocal-lattice points; they are narrow, quite clearly defined, and their strength varies little along their length; they join together to form plane sheets of scattering power, which are parallel to the c^* and to one of the a^* axes, and intersect along lines joining rows of reciprocal-lattice points parallel to the c^* axis.

(3) There is no sheet of scattering power lying along any a^* axis, or passing through the origin of the reciprocal lattice, though there are a few bridges, which make only a small angle with the a^* axes, which do not fall into this general scheme.

(4) The sheets pass through many 'forbidden' points, but at some other 'real' reciprocal-lattice points they show sharp discontinuities; they are not always centrosymmetrical about the reciprocal-lattice points.

(5) The diffuse pattern does not become broader or less clearly defined with increasing angle of reflexion.

The amplitudes of vibration of the molecules are of the order of 0·4 A. at $-5°$ C. The strong local disturbances which cause the diffuse streaks could include movements of the hydrogen atoms between neighbouring oxygen atoms.

Introduction

The diffuse scattering of X-rays by any crystal depends on the directions and amplitudes of the vibrations executed by the atoms, and these, in turn, depend upon the forces within and between the molecules. Ice is known to be molecular, but although the arrangement

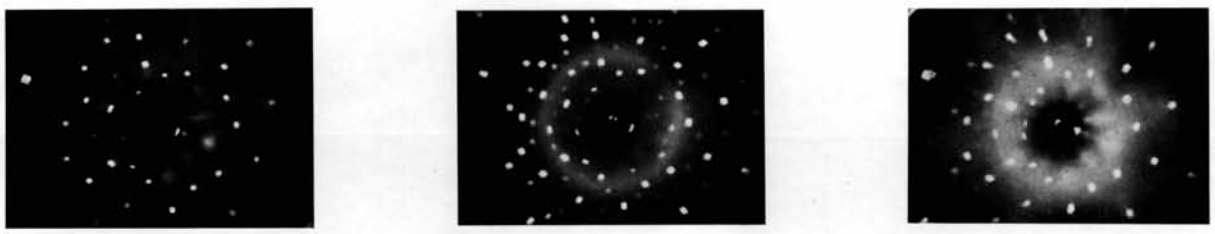

(*a*) (*b*) (*c*)

Fig. 1. Beam 4·6° from *c* axis (*a*) at −5° C., (*b*) cooled in liquid air, (*c*) temperature rising from −180 to −5° C.

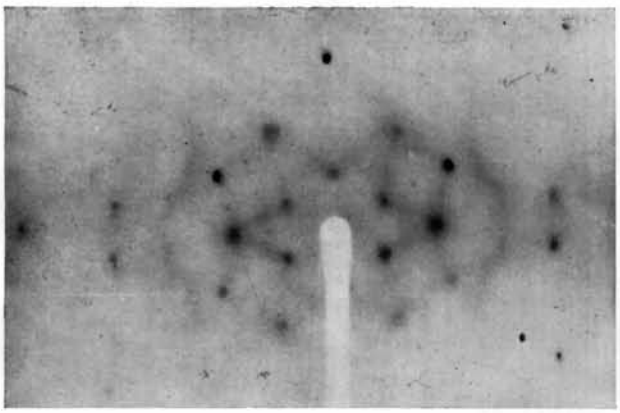

Fig. 2. Monochromatic Cu $K\alpha$ radiation along hexagonal axis. Exposure 4 hr.; −5° C.

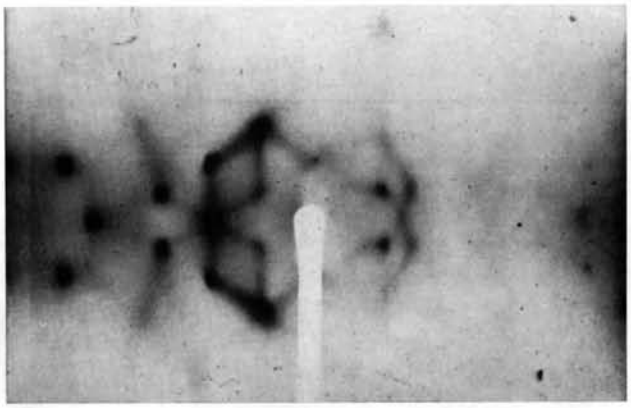

Fig. 3. Monochromatic Cu $K\alpha$ radiation 28° from *c* axis, [1$\bar{1}$†0] vertical. Exposure 4 hr.; −5° C. The rounded diffuse spots at the intersections of narrow streaks are well shown.

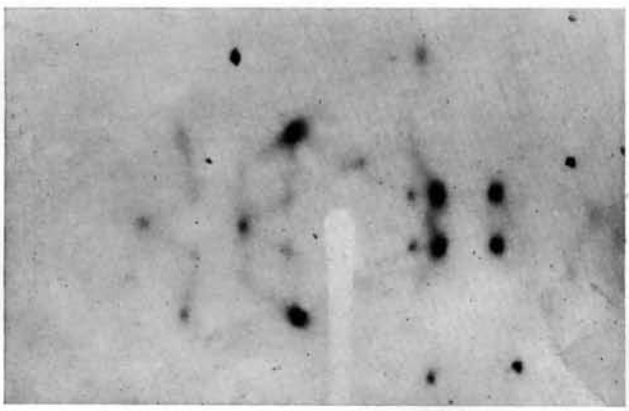

Fig. 4. Monochromatic Cu $K\alpha$ radiation 38° from *c* axis, [1$\bar{1}$†0] vertical. Exposure 4 hr.; −5° C.

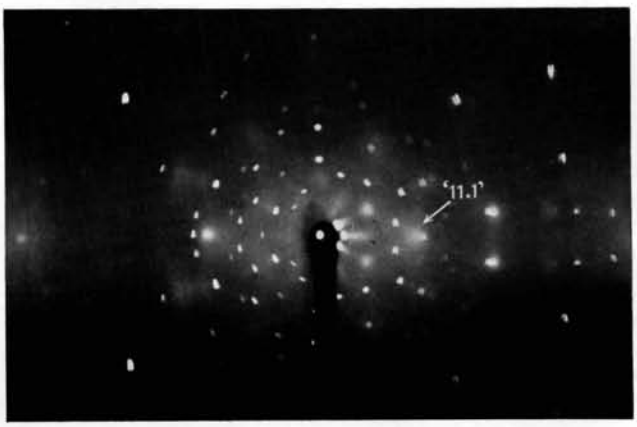

Fig. 5. Unfiltered Cu *K* radiation 4·9° from *c* axis, [1$\bar{1}$†0] approximately vertical. The diffuse reflexion in the 'forbidden' (11.1) position is shown.

[*To face p.* 222

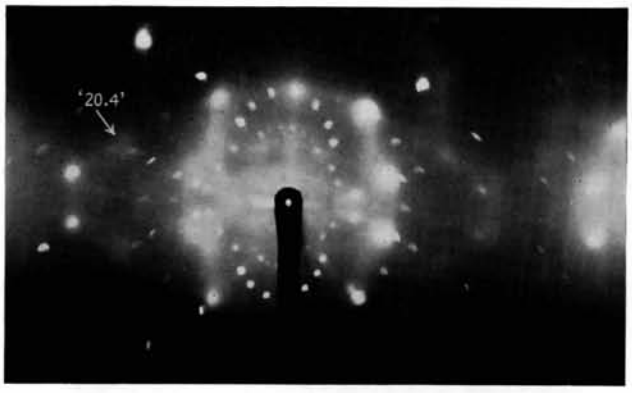

Fig. 6. Unfiltered Cu K radiation 86·8° from c axis, [1$\bar{1}$†0] approximately vertical. The diffuse reflexions include the 'forbidden' (20.4).

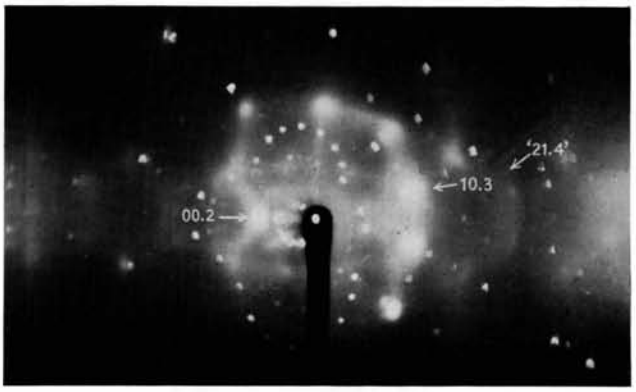

Fig. 7. Unfiltered Cu K radiation 82·3° from c axis, [1$\bar{1}$†0] approximately vertical. Besides the 'forbidden' (21.4) the strong diffuse reflexions from (00.2) and (10.3) are shown.

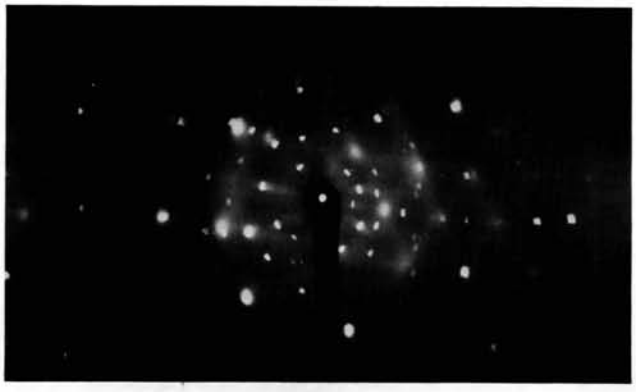

Fig. 8. Unfiltered Cu K radiation 45° from c axis, [10†0] 10° from vertical. The sphere of reflexion here cuts several sheets of scattering power, with diffuse spots at their intersections; the sheets are no broader at high angles of reflexion than lower angles.

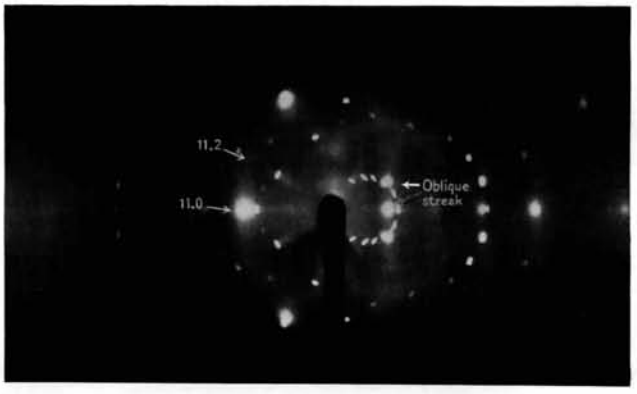

Fig. 9. Unfiltered Cu K radiation 13·5° from a axis, [00†1] vertical. The oblique streaks which do not fall into the general scheme are seen. A diffuse streak here passes from the (11.0) to near the (11.2) positions, passing through the 'forbidden' (11.1) position.

of oxygen atoms in ice I (normal ice) is well known and is comparatively simple, the positions and behaviour of the hydrogen atoms are not at all certain. It is generally assumed, however, that the hydrogen atoms lie along the O–O directions (one hydrogen only between each pair of oxygen atoms) and that the bonds thus formed, 2·76 A. in length, are typical hydrogen bonds, and are all of one kind.

The vibrations of the atoms in ice, therefore, may be regarded as typical of those associated with moderately long hydrogen bonds. Given the diffuse X-ray scattering, it should be possible, in theory at least, to deduce the amplitudes, frequencies and directions of these vibrations, and hence to gain useful information about the nature of the hydrogen bond. Ice, near to 0° C., gives particularly strong diffuse X-ray patterns, but so far it has not proved possible to do more than to draw some rather general conclusions from the experimental results, of which a comprehensive study has been made. The experimental results and the conclusions derived are given here partly because they embody a number of features to which attention has not previously been drawn in studies of this kind, and partly in the hope that they may stimulate further theoretical work in this general field.

Preparation of specimens

When water is frozen in the laboratory without special precautions the crystals formed are almost always too thin to be handled conveniently. Suitable specimens for diffuse X-ray scattering experiments were obtained by exposing photographic dishes of London tap water on cold days, or overnight, throughout the winters of 1945–6 and 1946–7. They were usually placed on a roof parapet to allow air to circulate freely. They were not protected from dust because any such protection hindered the free circulation of air and also generally resulted in supercooling. Crystallization usually began at a few centres on the surface, probably dust particles, from which needle-like crystals grew out rapidly across the surface; these were always too thin to be used. In time the surface became covered by a polycrystalline sheet of ice, which was allowed to grow until about 5 mm. thick. Quite often this happened overnight (although if the frost was really severe the whole of the water would freeze overnight and would be useless). The sheet of ice was then carefully removed, in one piece if possible, and was sometimes found to have crystals about 1 mm. thick and up to 2 cm. long growing from its under-surface. In the remaining liquid, crystals 2–3 mm. thick, 0·5–1 cm. broad and up to 10 cm. long were usually found floating. Sections of clear ice, free from included dust and air-bubbles, were cut from these crystals with a razor-blade and could be kept in the ice-making chamber of a refrigerator until needed, often for 2–3 months. Laue photographs showed most of these sections to be single, unstrained crystals. They had, however, no natural faces or good edges, and their only constant crystallographic property was that the length of the crystals was the $[1\bar{1}\dagger0]$ axis.

Various methods of mounting the crystals were tried. That finally adopted was to mount on arcs, by means of a short steel wire, a hollow brass block, $5 \times 9 \times 12$ mm., filled with cold water; the specimen, previously cooled by solid CO_2, was inserted in this, and the water was then frozen by touching the brass block with solid CO_2 for the minimum time necessary. Ice crystals crack very easily if left for too long in contact with solid CO_2. The crystal was finally trimmed with a razor-blade to a rough cylinder of 1–2 mm. diameter.

Description of experimental method

A few experiments were made using an improvised apparatus in which the crystal holder, mounted on a Müller spectrometer, was cooled by a small bath of alcohol and solid CO_2, the laboratory being kept as cold as possible (about 5° C.) by opening windows and doors.

Most of the results to be described, however, were obtained using the low-temperature camera designed by Cox (1932). This has a cylindrical film-holder of internal radius 4·44 cm. Alcohol, previously cooled by passing through a spiral tube immersed in a bath of alcohol and solid CO_2, was circulated between the double walls of the camera. On the more humid days it was necessary to pass a current of dry air through the camera to prevent moisture condensing on the specimen.

The X-ray tube used was a modified Shearer-type cold-cathode (gas) tube, passing an apparent 14 mA. at 45 kV. potential supplied by an induction coil and Newman electrolytic interruptor. By polishing the cathode and anode of the tube after every 4 hr. running, the emission intensity was kept at a maximum and the exposure times necessary with unfiltered radiation from a copper target were reduced to about $1\frac{1}{2}$ hr.

The crystals were set with the $[1\bar{1}\dagger0]$, $[10\dagger0]$ or $[00\dagger1]$ axis approximately vertical, but great accuracy in setting was not important, since the orientation of the crystals could be found exactly from the Laue pattern. Photographs were taken with the crystal stationary in as many different orientations as possible about each axis, at a temperature of about $-5°$ C.

A few exposures (time 4 hr.) were also made using radiation made monochromatic by reflexion from a crystal of urea nitrate.

Representation of results

In order to give a full description of the diffuse scattering from a crystal it would be necessary to determine its intensity in sufficient directions and with sufficient wave-lengths to give the distribution of scattering power throughout the whole of reciprocal space. This formidable task would not be justified in the present state of knowledge of crystal dynamics; a much simpler and more useful aim would be to locate

the regions of maximum scattering. This may be done by plotting the positions corresponding to the diffuse spots and streaks seen on the photographs.

The diffuse streaks radiating from the centres of many Laue photographs (Figs. 1–9) are due to the scattering of *white* radiation by atoms disturbed by thermal vibration. This may be proved by comparing,

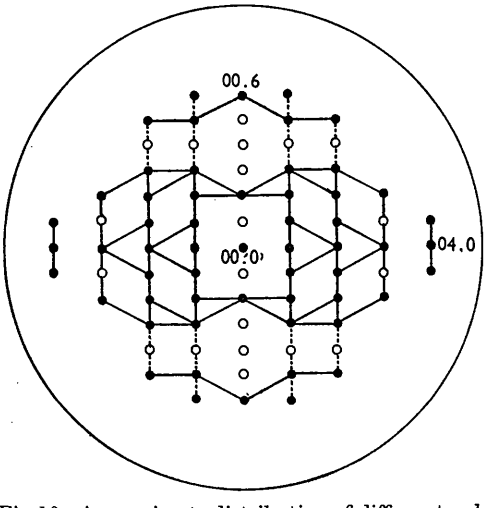

Fig 10. Approximate distribution of diffuse streaks in the layer $h=0$. Open circles: $F_{calc.}=0$. Closed circles: $F_{calc.}\neq 0$.

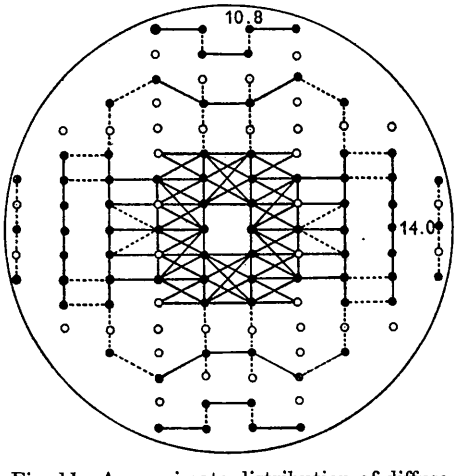

Fig. 11. Approximate distribution of diffuse streaks in the layer $h=1$.

for example, Fig. 1 (*a*) with Fig. 1 (*b*) and with Fig. 2, which show these streaks to be greatly reduced in intensity at low temperatures, and to vanish when monochromatic radiation is used. They will not be discussed further.

The diffuse spots and non-radial streaks which appear on the Laue photographs (see also Lonsdale, 1946) are due to the scattering of *characteristic* Cu K radiation by atoms moved from their mean positions by thermal vibration. This diffuse pattern practically disappears when the crystal is cooled in a stream of liquid air, and reappears when the crystal is warmed again (Fig. 1). It appears more clearly when monochromatic X-rays are used (Figs. 2–4).

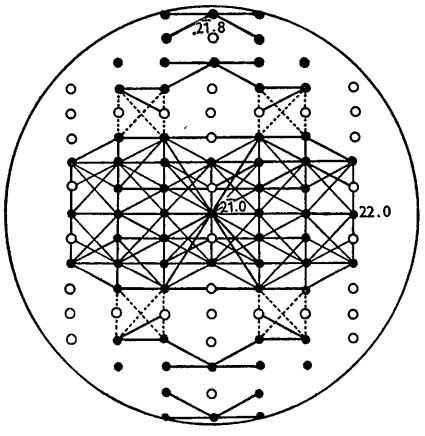

Fig. 12. Approximate distribution of diffuse streaks in the layer $h=2$.

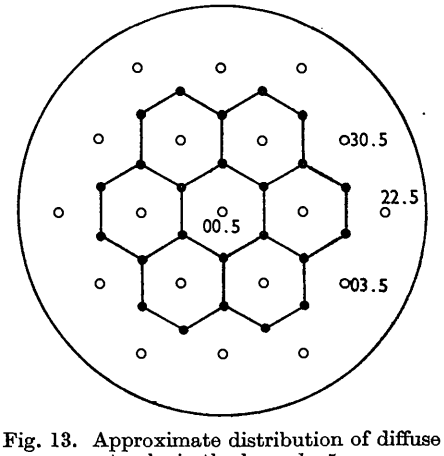

Fig. 13. Approximate distribution of diffuse streaks in the layer $l=5$.

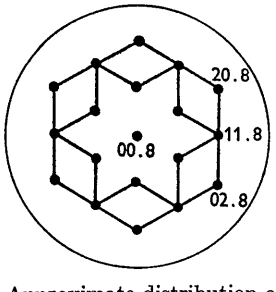

Fig. 14. Approximate distribution of diffuse streaks in the layer $l=8$.

The representation of diffuse scattering power in reciprocal space could therefore be carried out without difficulty by the use of the ordinary Ewald construction, since in each case a prominent crystal axis was nearly vertical. The diffuse spots were labelled with the indices of the nearest reciprocal-lattice point (see Lonsdale & Smith, 1941), and diffuse spots which were joined by diffuse streaks were tabulated. Diagrams, of the type

shown in Figs. 10–14, were then drawn, in which the reciprocal-lattice points with the indices listed were joined by straight lines. These diagrams are clearly inexact, for the diffuse spots are rarely in positions corresponding precisely to reciprocal-lattice points, and the streaks always correspond to arcs in reciprocal space and not to straight lines. Nevertheless, if these limitations are remembered, the distribution of scattering power is surprisingly well represented in this simple way. More precise information may be obtained by plotting in reciprocal space the exact positions corresponding to the diffuse spots. This has been done in Fig. 15 for the layer $l=0$, using some six photographs; the lengths of the short lines give the sizes of the diffuse spots when corrected for the size of the crystal and the divergence of the incident beam by subtracting the size of the corresponding Laue spots. On this diagram double dotted lines indicate the scattering maxima corresponding to the diffuse streaks. Figs. 16–18 similarly represent the distribution of diffuse scattering power in the levels $l=1, 2$ and 3 of the reciprocal lattice. It will be seen that Figs. 10–14 and 15–18 are complementary, and that the results of the two methods of plotting the maxima do not conflict, although the second series is more exact.

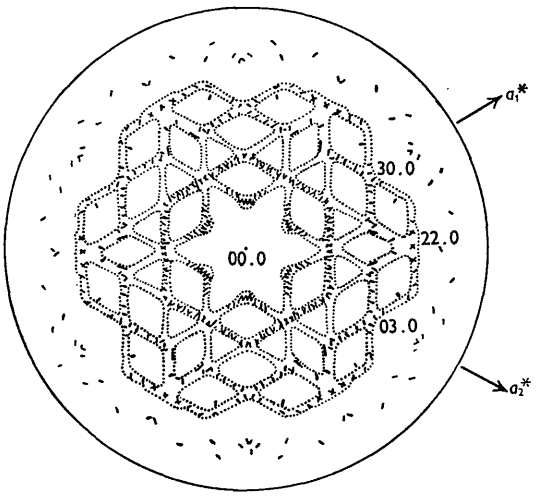

Fig. 15. Exact positions of the diffuse spots (heavy lines) and approximate positions of the diffuse streaks (dotted lines) in the layer $l=0$.

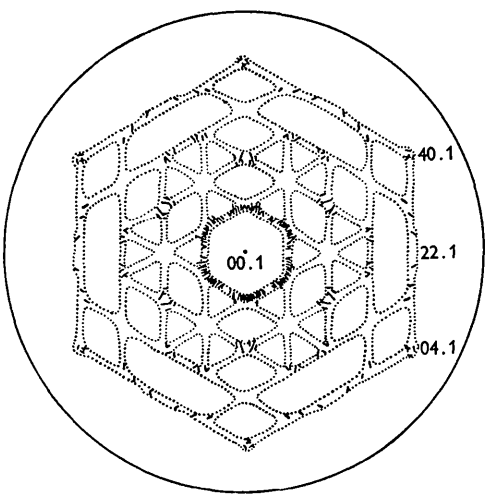

Fig. 16. Exact positions of the diffuse spots and approximate positions of the diffuse streaks in the layer $l=1$.

For one small area of the layer $h=1$ (Fig. 19, cf. Fig. 11), for which the observations were sufficiently complete, the positions in reciprocal space corresponding to both diffuse spots and streaks were carefully traced. This more precise representation, taken from eight photographs, shows that the main feature of Fig. 11, an apparently continuous sheet of scattering power with a well-marked clear area at the centre, is correct, and is not due to the approximations made in drawing Figs. 10–14.

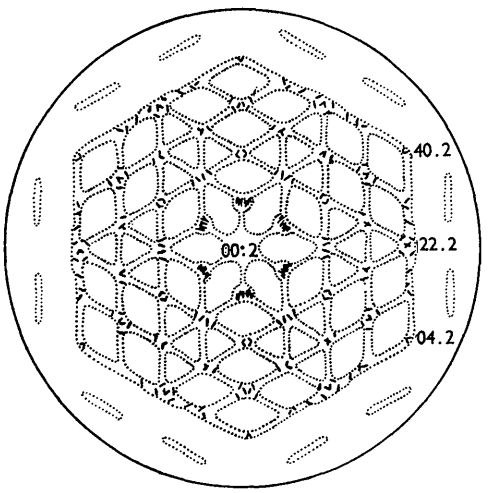

Fig. 17. Exact positions of the diffuse spots and approximate positions of the diffuse streaks in the layer $l=2$.

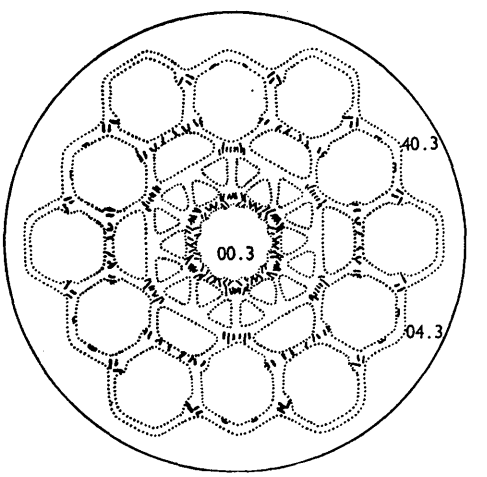

Fig. 18. Exact positions of the diffuse spots and approximate positions of the diffuse streaks in the layer $l=3$.

Discussion of results

A study both of these reciprocal-space diagrams and of the original photographs leads to the following description of the diffuse scattering power of ice just below the melting-point:

(*a*) The maximum scattering power is at and near to the reciprocal-lattice points and is best represented by rounded isodiffusion contours, quite unlike, for instance, those of sodium (Lonsdale & Smith, 1942; Jahn, 1942; Lonsdale, 1943). In intensity, however, the diffuse spots are comparable with those of sodium. Now calculations from specific-heat data show that the root-mean-square amplitude of thermal vibration of sodium atoms at room temperatures is about 0·5 A. (Lonsdale, 1948), and the anisotropy of the diffuse pattern from sodium shows that in some directions the amplitudes of vibration must be much greater than this mean value. Atomic movements of similar amplitudes must also occur in ice near to its melting point. An approximate calculation from the values of the specific heat at low temperatures given by Giauque & Stout (1936), strictly only applicable to cubic crystals, gives a characteristic temperature of 192° K. and a root mean square amplitude of vibration of the water molecules of 0·42 A. at −5° C.

(*b*) Away from the reciprocal-lattice points the scattering power is found to occur in sheets which coincide with the nets of reciprocal-lattice points $h,k,i=1,2,3,\ldots$ (but not 0). These sheets intersect along rows of reciprocal-lattice points parallel to the c^* axis, and it may be seen from Fig. 19 that diffuse spots often occur in positions corresponding to points along the lines of intersection of the sheets, while the streaks correspond to intersection of the sheets by the sphere of reflexion.

(*c*) The sheets are not continuous, but show gaps, especially around the origin of the reciprocal lattice. One important corollary of this fact, which any theory of diffuse scattering must explain, is that the diffuse scattering power is not distributed centrosymmetrically in the neighbourhood of strongly reflecting reciprocal-lattice points. The points (10.0), (10.1), (10.2), which lie on the boundary of the clear zone in the centre of the reciprocal lattice, all have very large structure factors.

(*d*) In addition, the scattering power is not always zero at reciprocal-lattice points whose calculated structure factors are zero. Thus when crystals were orientated so as to fulfil the Bragg condition for the planes (11.1) (Fig. 5), (20.4) (Fig. 6), (21.4) (Fig. 7), (22.3) and (11.3), the positions on the photographs where Bragg reflexions would have appeared if the structure factors had not been zero were occupied by diffuse spots, with diffuse streaks passing through them. This is also almost certainly true for the planes (30.1) and (11.5), although in the photographs concerned here the Bragg condition was not quite exactly fulfilled. If a series of photographs is studied, such as those used in constructing Fig. 19, it is found that the diffuse spot which moves from the (11.0) to the (11.2) selective reflexion positions, passing through the 'forbidden' (11.1) position in doing so, actually varies very little in intensity, except that it is very much stronger in the immediate neighbourhood of the two 'real' reflexion positions.

This effect appears not to have been reported previously. Its explanation must lie in the fact that the thermal vibrations are of such a kind that the scattering from the atoms, which would cancel out for these particular reflexions if the atoms were at rest, does not cancel out when they are moving. The structure factor, modified by temperature, is no longer zero for these planes, and therefore diffuse scattering occurs. This is a special case of the fact (Stokes, 1948) that the phase angles of reflexions from a crystal which is not at absolute zero are not, in general, exactly 0 or $\pm\pi$, even for crystals with an average centrosymmetrical structure.

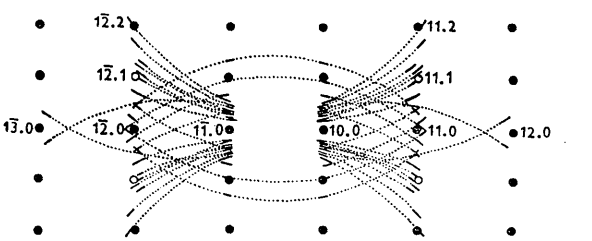

Fig. 19. Exact positions of the diffuse spots (heavy lines), and of the diffuse streaks (dotted lines) in the layer $h=1$.

No diffuse scattering was observed in positions corresponding to the 'forbidden' Bragg reflexions (00.l) with l odd, and very little was observed for the net $l=4$, except for the two planes mentioned above, (20.4) and (21.4), and a few weak streaks marked as dotted lines in Figs. 11 and 12. The thermal vibrations must therefore be such as to leave the 'extinction conditions' unaffected for these reflexions.

(*e*) It is important to notice that there is no sheet of scattering power which passes through the origin itself; the extension of scattering power along the a^* axes is limited to the strong concentrations immediately around the reciprocal-lattice points. There are a few bridges, which do not fall into the general scheme, which make only a small angle with the a^* axes. They are shown in Fig. 10, in which only the vertical lines, which represent the intersections of sheets, are part of the system here described; the horizontal and oblique lines are not. Some of the corresponding oblique streaks may be seen in Fig. 9.

(*f*) It is shown particularly clearly in Fig. 4 that the diffuse streaks, and hence the sheets of scattering power which correspond to them in reciprocal space, are comparatively narrow and clearly defined. Their intensity is constant along their length, showing neither maxima nor minima near the mid-points, which should

correspond to high-frequency vibrations causing considerable relative movement of neighbouring atoms. Moreover, diffuse spots and streaks at high angles of reflexion, corresponding therefore to small-spacing planes, are hardly, if at all, broader or less clearly defined than those at low angles (see also Fig. 8).

Inadequacy of existing theory

In the case of the cubic metals Na, Li, Pb, W, and of the alkali halides, the theory given by Faxén and Waller, and developed by Jahn, Born and others (see Born (1942–43)), is adequate to give a reasonably satisfactory explanation of the experimental observations (Lonsdale, 1942–43, 1943). That is not the case for ice. A theory of the diffuse X-ray scattering to be expected in close-packed hexagonal crystals subject to thermal vibrations has been given by Begbie (1947), the assumption being made that only next-neighbour atoms act on one another. The formulae given have been found to fit the experimental data for beryl and zinc fairly well (Lonsdale, unpublished). They require a knowledge of the elastic constants, which are not adequately known for ice; values which are reasonably consistent with the best available determinations of the elastic moduli (Northwood, 1947; Richards & Speyers, 1914) are

$$C_{33} \approx C_{11} = 14{\cdot}7 \times 10^{10} \text{ dyne cm.}^{-2},$$

$$C_{13} \approx C_{11} = 7{\cdot}35 \times 10^{10} \text{ dyne cm.}^{-2},$$

and

$$C_{66} \approx C_{44} = 3{\cdot}68 \times 10^{10} \text{ dyne cm.}^{-2}.$$

Using these constants, and using the value of 0·4 A. for the root-mean-square amplitude of vibration of the oxygen atoms in the Debye temperature factor $M = 8\pi^2\overline{u^2}(\sin\theta/\lambda)^2$, Begbie's equations lead to the isodiffusion contours shown in Fig. 20 for the layer $l=0$ of the reciprocal lattice. Since only long waves are considered in the calculations, the results apply only to scattering very near the reciprocal-lattice points. There they predict, as is found experimentally, rounded isodiffusion contours, with the intensity of diffuse scattering varying little with the angle of reflexion, apart from the very intense (10.0) and (11.0) reflexions. The shape of the contours is not very sensitive to variations in the elastic constants used, and no combination whatever of elastic constants would explain the strong and comparatively even sheets of diffuse scattering, and the asymmetry of these sheets with respect to certain reciprocal-lattice points having large structure factors.

The explanation of the diffuse streaks must therefore be sought in disturbances which are not long harmonic waves. Thin sheets of diffuse scattering lying in the directions found for ice could be due to transverse waves travelling in all directions in the (11.0) planes. Since all the O–O bonds lie in these planes, the atoms would then vibrate perpendicular to the O–O bonds. The sharp asymmetry about the (10.0) and (11.0) reciprocal-lattice points, however, remains unexplained.

Local disturbances which could be propagated along the bonds are rotation of the molecules, and movements of the hydrogen atoms between their two equilibrium positions, ~1 A. from each oxygen atom. These were suggested by Pauling (1935) to explain the physical properties of ice. Rotation of the molecule would move the oxygen atom very little from its mean position; proton transfer, however, requires neighbouring oxygen atoms to move towards each other by at least 0·1 A. (Huggins, 1936). Movements of this amplitude could well be among those responsible for the diffuse streaks.

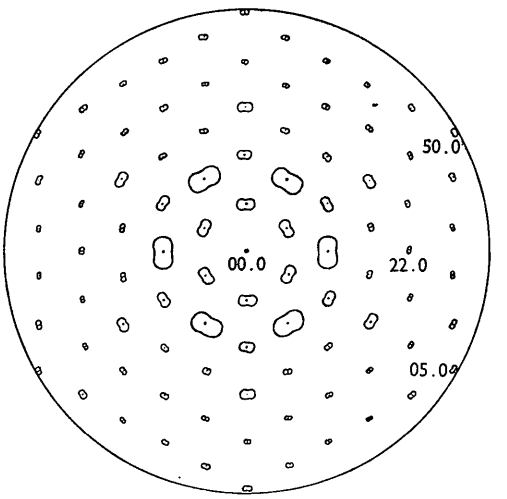

Fig. 20. Isodiffusion contours for the layer $l=0$, calculated from elastic constants.

These strong local disturbances, of course, are not peculiar to ice. Diffuse streaks are given by other substances, e.g. NaCl (Gregg & Gingrich, 1941), Na (Lonsdale, 1942) and KCl (Guinier, 1945), though no full experimental study of them has been made. The calculations of Begbie & Born (1947) on sylvine suggest that it may be possible to explain diffuse streaks by a further development of the theory so as to include vibrations of shorter wave-lengths, but for hexagonal crystals this has not yet proved possible.

The author wishes to thank the Managers of the Royal Institution for making available the facilities of the Davy-Faraday laboratory, and the Agricultural Research Council for a grant which enabled him to carry out the investigation.

He is greatly indebted to Dr Kathleen Lonsdale for her help and advice throughout the work.

References

Barnes, W. H. (1929). *Proc. Roy. Soc.* A, **125**, 670.
Begbie, G. H. (1947). *Proc. Roy. Soc.* A, **188**, 189.
Begbie, G. H. & Born, M. (1947). *Proc. Roy. Soc.* A, **188**, 179.
Born, M. (1942–43). *Rep. Phys. Soc. Progr. Phys.* **9**, 294.
Cox, E. G. (1932) *Proc. Roy. Soc.* A, **135**, 49.

GIAUQUE, W. F. & STOUT, J. W. (1936). *J. Amer. Chem. Soc.* **58**, 1144.
GUINIER, A. (1945). *Proc. Phys. Soc.* **57**, 310.
GREGG, R. Q. & GINGRICH, N. S. (1941). *Phys. Rev.* **59**, 619.
HUGGINS, M. L. (1936). *J. Phys. Chem.* **40**, 723.
JAHN, H. A. (1942). *Proc. Roy. Soc.* A, **179**, 320.
LONSDALE, K. (1942–43). *Rep. Phys. Soc. Progr. Phys.* **9**, 256.
LONSDALE, K. (1943). *Proc. Phys. Soc.* **54**, 314.
LONSDALE, K. (1946). *Nature, Lond.*, **158**, 582.
LONSDALE, K. (1948). *Acta Cryst.* **1**, 142.
LONSDALE, K. & SMITH, H. (1941). *Proc. Roy. Soc.* A, **179**, 8.
LONSDALE, K. & SMITH, H. (1942). *Nature, Lond.*, **149**, 21.
NORTHWOOD, T. D. (1947). *Canad. J. Res.* **25**A, 88.
PAULING, L. (1935). *J. Amer. Chem. Soc.* **57**, 2680.
RICHARDS, T. W. & SPEYERS, C. L. (1914). *J. Amer. Chem. Soc.* **36**, 491.
STOKES, A. R. (1948). *Nature, Lond.*, **161**, 679.

Acta Cryst. (1949). **2**, 228

The Crystal Structure of Aniline Hydrochloride

BY C. J. BROWN

Research Laboratories, Imperial Chemical Industries Limited (Dyestuffs Division), Hexagon House, Blackley, Manchester 9, Great Britain

(*Received* 17 *March* 1949)

The crystal structure of aniline hydrochloride has been determined by the X-ray method. The space group is *Cc*, with cell dimensions $a = 15{\cdot}84 \pm 0{\cdot}03$, $b = 5{\cdot}33 \pm 0{\cdot}03$, $c = 8{\cdot}58 \pm 0{\cdot}03$ A., $\beta = 101° \pm 30'$. $\rho_{exp.} = 1{\cdot}210$, while that required for four molecules per unit cell is 1·211. X-ray intensities were obtained from Weissenberg photographs taken of the zero levels about [*a*], [*b*] and [*c*]. The trial structure was found by means of a Patterson projection along [*b*], and this was refined by means of successive two-dimensional Fourier syntheses. The structure is ionic, each nitrogen atom being equidistant at 3·17 A. from three chlorine ions. The dimensions of the benzene ring are normal, but the C–N bond is considerably shorter (1·35 A.) than that given by the sum of the atomic radii (1·47 A.).

Introduction

In all the crystal structures of aromatic amines which have been determined, the C–NH_2 bond has been found to be considerably shorter than that to be expected from the sum of the atomic radii of carbon and nitrogen. This shortening has been observed in a wide variety of aliphatic compounds as well as aromatic, and some of the published values of the C–N bond length are listed in Table 3. The crystal structure of acetanilide (Brown & Corbridge, 1948) also revealed a low value for the C–N bonds, and it was during the course of this work that interest was first aroused in the structure of aniline hydrochloride. It was considered possible that in some of the compounds listed in Table 3, the short C–N bond might be due to the influence of other substituents in the benzene ring; further, the only simple amine which has been attempted is *p*-toluidine (Wyart, 1935), and the C–N bond value obtained for that substance (1·18 A.) was so low that its reliability may be doubtful. For these reasons, it was decided to work out the structure of aniline hydrochloride in order to obtain more data regarding the bond lengths in amines.

Experimental

Crystals of aniline hydrochloride grown from ethanol exhibited a pronounced platy development, and were not very suitable for obtaining accurate X-ray intensities. In addition, very perfect cleavage parallel to (100) and (011) rendered the production of suitable crystal shapes by grinding or cutting impossible, so it was necessary to choose fairly small crystal fragments to minimize absorption errors.

The dimensions of the unit cell were obtained by measurement of the layer lines of rotation photographs. The monoclinic angle was obtained by calculation from the unit lengths of [*a*], [*c*] and [101]:

$$a = 15{\cdot}84 \pm 0{\cdot}03, \quad b = 5{\cdot}33 \pm 0{\cdot}03,$$
$$c = 8{\cdot}58 \pm 0{\cdot}03 \text{ A.}, \quad \beta = 101° \pm 30'.$$

For four molecules per unit cell the specific gravity required is 1·211, while that observed experimentally by flotation is 1·210. Observed extinctions were $\{hkl\}$ for $(h+k)$ odd and $\{h0l\}$ for l odd, whence the space group may be either *Cc* or *C*2/*c*. As only four molecules are present in the cell, the space group *C*2/*c* would require the twofold axis of the aniline molecule to be parallel to [*b*]. As [*b*] is 5·33 A., this is clearly impossible, assuming standard bond lengths and angles, so the space group is determined without ambiguity as *Cc*.

Weissenberg moving-film photographs were taken of the zero levels of the *a*, *b* and *c* axes, using a modified multiple-film technique with batches of six films. The intensities of the spots were estimated visually by comparison between the batches of films. The absorp-